SELECTIVE HARMONIC ELIMINATION IN PULSEWIDTH MODULATION INVERTERS USING GENETIC ALGORITHM

A REPORT

submitted by

SREE SUBIKSHA. M. R

in partial fulfilment of the requirements

for the award of the degree

of

BACHELOR OF TECHNOLOGY

DEPARTMENT OF ELECTRICAL ENGINEERING

INDIAN INSTITUTE OF TECHNOLOGY MADRAS

May 2018

CERTIFICATE

This is to certify that the report titled **Selective Harmonic Elimination in Pulsewidth Modulation Inverters using Genetic Algorithm**, submitted by **Ms. Sree Subiksha. M. R**, to the Indian Institute of Technology Madras, in partial fulfilment of the requirements for the award of the degree of **Bachelor of Technology** is a bonafide record of the work done by her under my supervision. The contents of this report, in full or in parts, have not been submitted to any other Institute or University for the award of any degree or diploma.

Place : Chennai

Dr. Mahesh Kumar
Professor
Department of Electrical Engineering
Indian Institute of Technology Madras

ACKNOWLEDGEMENTS

I would like to express my profound gratitude to my project supervisor Dr. Mahesh Kumar. I am very fortunate to have worked under his guidance. His vast knowledge, outlook towards research, patience and willingness to help, has enriched me as a researcher and as a person.

I also owe my thanks to the faculty of the Power group. The wonderful undergraduate and graduate level courses offered by the faculty inspired me to choose Power Engineering as a field to do my undergraduate project. I thank all my fellow project mates and research scholars in the Power Quality laboratory for having supported and helped me during the course of the project.

I am thankful to my family and friends at IIT Madras, who have always unconditionally supported and encouraged me. I thank the IIT Madras community for the great experience in this institute. Above all, I thank the Almighty for the person that I am today.

Sree Subiksha. M. R

ABSTRACT

Keywords: Pulsewidth modulation inverter, Programmed pulsewidth modulation, selective harmonic elimination, genetic algorithm

Pulsewidth modulation inverters are used in several applications. A major operating consideration of the PWM inverters is the high harmonic content in their output spectra. The inverters must be operated at high switching frequencies to push the harmonics in their output spectra to higher frequencies such that they can be easily filtered by a passive filter. However, high switching frequency of the inverter results in large power loss. Therefore, the focus has now shifted on investigating means to suppress the harmonics in the output spectrum of the inverter while at the same time maintaining low switching frequencies.

A possible solution to the harmonics mitigation problem while maintaining low switching frequencies is the programmed PWM scheme. In programmed PWM schemes, the switching angles of the PWM output voltage waveforms are pre-calculated. The values of the switching angles are such that, in the Fourier series expansion of the PWM output voltage waveform, the magnitudes of all the undesired harmonics is reduced to zero. This is called selective harmonic elimination (SHE). The determination of the switching angles that satisfy the SHE criteria is a constrained global optimization problem. If the number of harmonics to be eliminated is N-1, this problem requires the solving of *N* simultaneous nonlinear equations to determine the values of *N* switching angles in one quarter cycle.

In this work, the simultaneous nonlinear equations associated with selective harmonic elimination in PWM inverters are solved using the genetic algorithm, an evolutionary algorithm capable of solving global optimization problems.

TABLE OF CONTENTS

LIST OF TABLES

LIST OF FIGURES

ABBREVIATIONS

EA	Evolutionary Algorithm
FACTS	Flexible AC Transmission System
GA	Genetic Algorithm
PWM	Pulsewidth Modulation
SHE	Selective Harmonic Elimination
SVC	Static VAR Compensator
UPS	Uninterrupted Power Supply
VSI	Voltage Source Inverter

CHAPTER 1

INTRODUCTION

The usage of power electronic has increased tremendously in the 21st century and we further expect to see an extension to the use of power electronics in many more applications [1]. This increase in the use of power electronics has been in both industrial and consumer applications. Power electronics is also an important component of modern high-efficiency energy processing systems, such as HVDC, SVC, FACTS for active and reactive power flow control, uninterruptible power supply (UPS), and industrial process control with variable-frequency drives for improving productivity and quality of products in modern automated factories [2].

Power electronics-based equipment connected to the electric grid are predominantly either power electronics-based loads or interfacing equipment such as inverters used for coupling renewable energy supplies with the grid [3], or those used in grid connected active power filters. Grid-connected power electronics-based equipment draw non-sinusoidal distorted current from the grid, thereby distort the grid-side voltage, and result in the flow of harmonic currents in the system. The flow of harmonic currents in the system can overload electrical distribution equipment, resonate with power factor correction capacitors, and cause connected rotating loads to heat up. Another important application of power electronics is that of inverters used in motor drives. The inverter output voltage must be sufficiently filtered before supplying to the motor as it is rich in harmonic content and can thereby cause the motor to significantly heat up.

1.1 PULSEWIDTH MODULATION INVERTERS

Almost all power electronics-based equipment, except for a few equipment that are used solely for rectification purposes use pulsewidth modulation inverters [4]. PWM inverters

are power electronics-based inverters whose output voltage profile is controlled by providing appropriate pulsewidth modulated gating signals to the inverter switches.

1.1.1 Reducing the harmonic currents injected by PWM inverters

Two major approaches are adopted collectively to reduce the harmonic currents injected by PWM inverters. The first approach is associated with coupling the inverter to the load or grid using passive filters [5]. This is shown in Figure 1.1. The interfacing filter attenuates high frequency components of the current injected. The second approach is associated with adopting appropriate control schemes for the PWM inverters to mitigate the harmonics content in the inverter output end voltage. The voltage profile at the output end of the PWM inverters, the end that is connected to the load or coupled with the grid, determines the nature of the current injected by the inverter. Improved voltage quality at the inverter output end directly improves quality of the current injected.

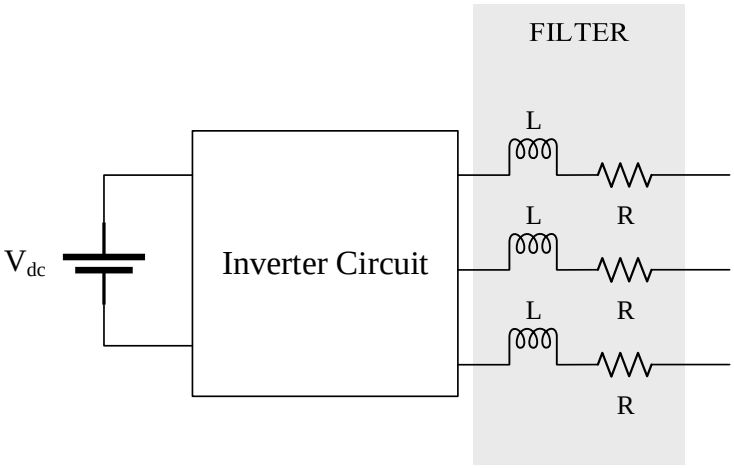

Figure 1.1. RL filter connected to the inverter output terminals

1.1.2 Control Schemes of PWM Inverters

The control schemes of PWM inverters are broadly classified as **carrier-based sinusoidal PWM schemes** and **programmed PWM schemes** [6]. Carrier-based sinusoidal PWM schemes involve the generation of gating signals for inverter switches by comparing the

instantaneous magnitudes of an ideal (sinusoidal) reference waveform and a high frequency carrier waveform. In this scheme, the switching frequency is the frequency of the carrier waveform.

In programmed PWM schemes, the switching angles of the inverter output voltage waveform are pre-computed. These are determined to optimize particular objective functions associated with improving the performance characteristics of the inverter. Improving the performance characteristics of the inverter is directly linked to decreasing the harmonic content in the output spectra of the inverter, especially the magnitudes of the low order harmonics. Therefore, the various objective functions chosen to generate programmed PWM in a generic sense constitute the elimination of low order harmonics in the inverter output spectra. This is called selective harmonic elimination (SHE).

The determination of the switching angles boils down to solving a set of nonlinear transcendental equations, whose number is one more than the number of harmonics required to be eliminated. The one additional equation is used to provide control over the magnitude of the fundamental component of the output voltage waveform. The nonlinear transcendental equations are obtained by equating the magnitude of all undesired harmonic components to zero and setting the desired magnitude to the fundamental component.

1.1.3 Advantages of SHE-based Programmed PWM

SHE-based Programmed PWM schemes provide a considerably improved harmonics profile at the output end of the inverter as compared to carrier-based PWM schemes. In carrier based PWM, there is effectively no control over the magnitudes of the non-fundamental frequency components of the output voltage. Inverters operated using carrier-based PWM schemes require considerably large coupling inductors to provide a similar attenuation in low order odd harmonics. The large coupling inductances are not only physically bulky but have another drawback that they significantly regulate the fundamental component of the output voltage. Also, programmed PWM schemes operate at much lower switching frequencies than carrier-based PWM schemes, thereby tremendously reducing the stress on the inverter switches and lowering the total power loss.

1.2 ORGANIZATION OF REPORT

In **Chapter 1**, the problems related to harmonic currents associated with the operation of power electronics-based equipment are discussed. Adopting appropriate control schemes for PWM inverters in power electronics-based equipment is seen as a possible solution to mitigating the harmonic currents injected by the equipment. Programmed PWM schemes are discussed and their ability to produce SHE in the output voltage waveforms of PWM inverters is introduced. The advantages of programmed PWM schemes over traditional carrier-based PWM schemes are discussed.

In **Chapter 2**, the classification of the various programmed PWM schemes is discussed. The nature of the output PWM voltage waveforms produced by various PWM schemes for the half-bridge, full-bridge and three-phase inverters is analysed in detail and the Fourier series expansion of the output voltage waveforms is discussed. The details of the harmonics required to be eliminated for the different schemes is discussed.

In **Chapter 3**, the requirement of an evolutionary algorithm-based optimization approach to solve for the switching angles for SHE in programmed PWM is discussed. The implementation of the genetic algorithm, an evolutionary algorithm is discussed. The global optimization problem of determining the optimized switching angles for various programmed PWM schemes is formulated and solved using the genetic algorithm. The trend followed by the optimized values of the switching angles with respect to the modulation index is observed.

In **Chapter 4**, the conclusions of the work conducted are presented. Selective harmonic elimination of undesired low order harmonics in the inverter output spectra using programmed PWM is possible. The technique of mitigating high order harmonics that remain uneliminated by the programmed PWM schemes using passive filters is mentioned.

CHAPTER 2

CLASSIFICATION OF PROGRAMMED PWM SCHEMES

Programmed PWM schemes are classified according to the inverter topologies in which they are deployed and the nature of the associated PWM output voltage waveforms. The schemes are discussed in detail below. The PWM output voltage waveform (for an ideal sinusoidal reference) generated using the schemes below has odd and quarter-wave symmetries. Therefore, all odd harmonics and cosinusoidal components are absent in the output voltage waveform.

The magnitude of the DC link voltage supporting the inverters is V_{dc}. The switching angles in the first quarter cycle are $\alpha_1, \alpha_2, \alpha_3 \ldots \alpha_N$. The output voltage switches from one of the allowed levels to another of the allowed levels at the switching angles. The values of the *N* switching angles in the first quarter cycle are sufficient to determine the switching pattern for the entire cycle since the waveform has odd and quarter-wave symmetries.

2.1 PWM SCHEMES FOR THE HALF-BRIDGE INVERTER

The half-bridge inverter configuration is given in Figure 2.1. The PWM output voltage waveform for this inverter configuration has two switching levels, $+\frac{V_{dc}}{2}$ and $-\frac{V_{dc}}{2}$. The values of the inverter switching angles are determined to eliminate the low order odd harmonics, i.e. the 3rd, 5th, 7th, 9th… harmonics are eliminated in the output voltage waveform.

2.1.1 Single phase bipolar scheme A

The PWM output voltage waveform representing one sinusoidal cycle begins with a magnitude of $-\frac{V_{dc}}{2}$ at phase 0°. The nature of the output voltage waveform for odd and even number of switching angles per quarter cycle is given in Figure 2.2 and Figure 2.3 respectively.

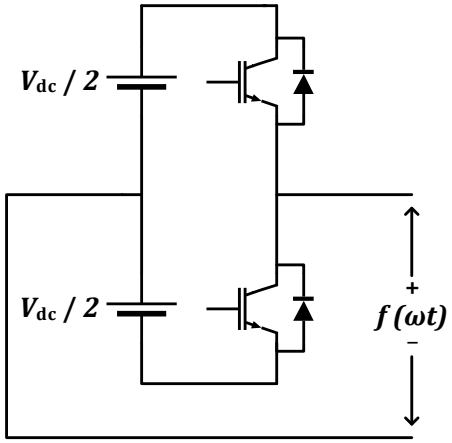

Figure 2.1. Half-bridge inverter configuration

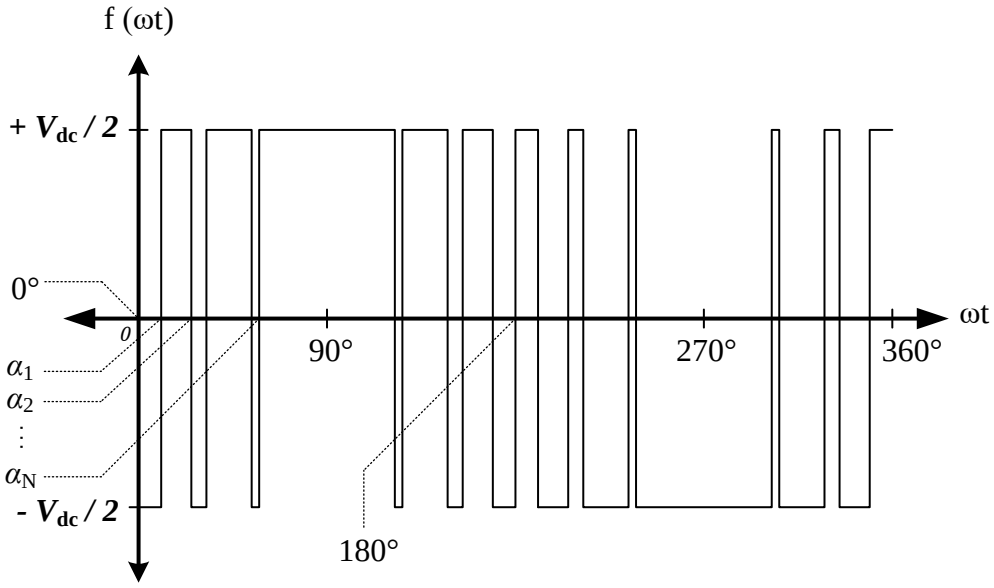

Figure 2.2. PWM output voltage waveform for bipolar scheme A in the half-bridge inverter (odd number of switching angles per quarter cycle)

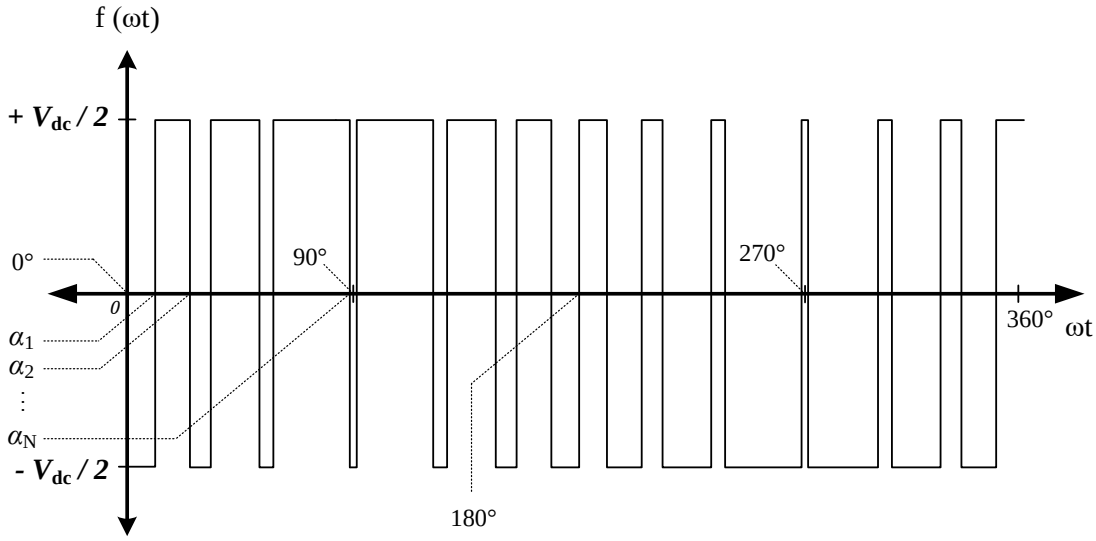

Figure 2.3. PWM output voltage waveform for bipolar scheme A in the half-bridge inverter (even number of switching angles per quarter cycle)

The Fourier series expansion of the output voltage waveform is given below.

$$f(\omega t) = \sum_{n=1,3,5,7\ldots} -\frac{2V_{dc}}{n\pi}\left[1 + 2\sum_{r=1}^{N}(-1)^r \cos(n\alpha_r)\right]\sin(n\omega t)$$

2.1.2 Single phase bipolar scheme B

The PWM output voltage waveform representing one sinusoidal cycle begins with a magnitude of $+\frac{V_{dc}}{2}$ at phase 0°. The nature of the output voltage waveform for even and odd number of switching angles per quarter cycle is given in Figure 2.4 and Figure 2.5 respectively.

The Fourier series expansion of the output voltage waveform is given below.

$$f(\omega t) = \sum_{n=1,3,5,7\ldots} \frac{2V_{dc}}{n\pi}\left[1 + 2\sum_{r=1}^{N}(-1)^r \cos(n\alpha_r)\right]\sin(n\omega t)$$

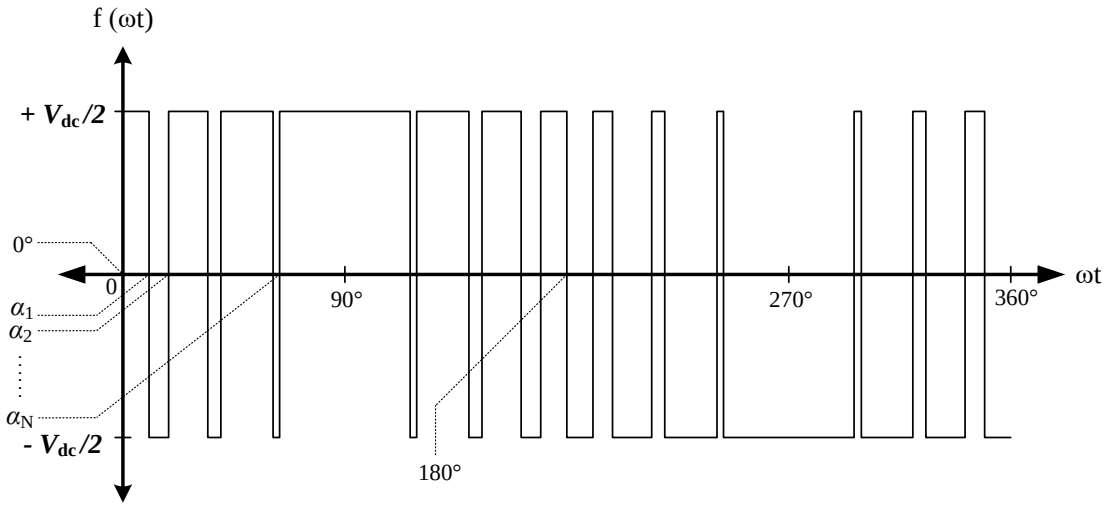

Figure 2.4. PWM output voltage waveform for bipolar scheme B in the half-bridge inverter (even number of switching angles per quarter cycle)

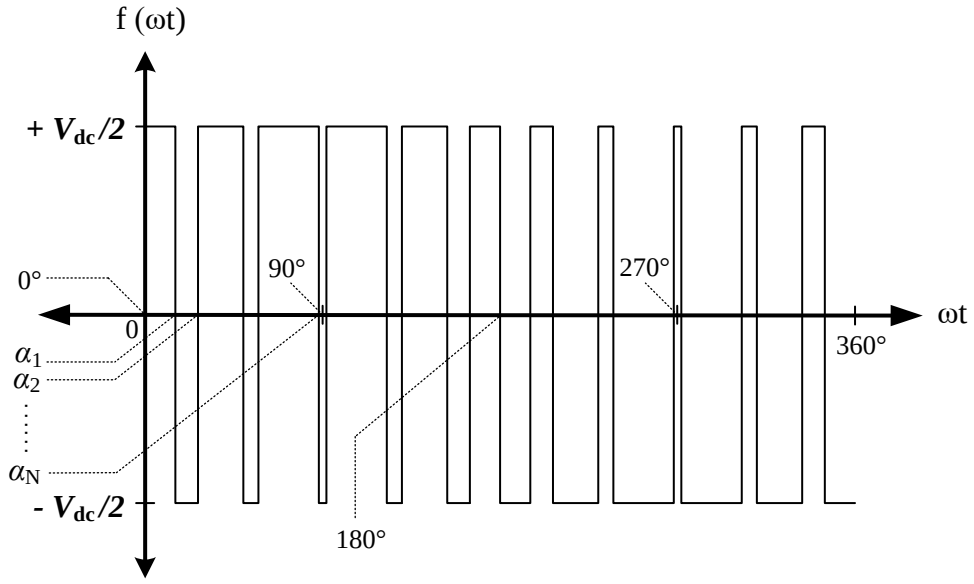

Figure 2.5. PWM output voltage waveform for bipolar scheme B in the half-bridge inverter (odd number of switching angles per quarter cycle)

2.2 PWM SCHEMES FOR THE FULL-BRIDGE INVERTER

The full-bridge inverter configuration is given in Figure 2.6. The values of the inverter switching angles are determined to eliminate the low order odd harmonics, i.e. the 3rd, 5th, 7th, 9th … harmonics are eliminated in the output voltage waveform.

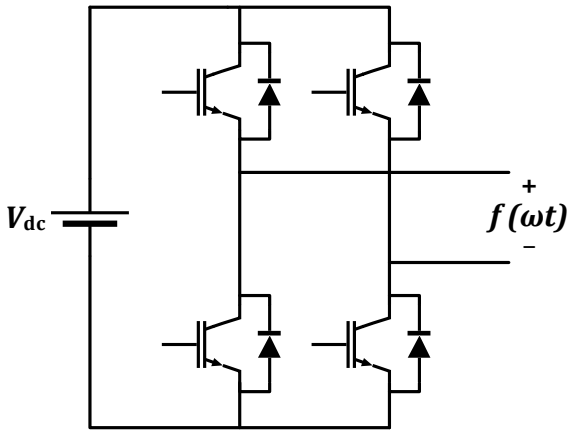

Figure 2.6. Full-bridge inverter configuration

2.2.1 Single phase bipolar scheme A

The PWM output voltage waveform has 2 switching levels, $+V_{dc}$ and $-V_{dc}$. The gating signals for the switches in the two inverter legs are the inverse of each other. The PWM output voltage waveform representing one sinusoidal cycle begins with a magnitude of $-V_{dc}$ at phase 0°. The output voltage waveform generated is the same as the output voltage waveform generated by the bipolar PWM scheme A in the half-bridge inverter (with the same DC link voltage), scaled by a factor of 2.

The Fourier series expansion of the output voltage waveform is given below.

$$f(\omega t) = \sum_{n=1,3,5,7\ldots} -\frac{4V_{dc}}{n\pi}\left[1 + 2\sum_{r=1}^{N}(-1)^r \cos(n\alpha_r)\right]\sin(n\omega t)$$

2.2.2 Single phase bipolar scheme B

The PWM output voltage waveform has 2 switching levels, $+V_{dc}$ and $-V_{dc}$. The gating signals for the switches in the two inverter legs are the inverse of each other. The PWM output voltage waveform representing one sinusoidal cycle begins with a magnitude of $-V_{dc}$ at phase 0°. The output voltage waveform generated is the same as the output voltage waveform generated by the bipolar PWM scheme A in the half-bridge inverter (with the same DC link voltage), scaled by a factor of 2.

The Fourier series expansion of the output voltage waveform is given below.

$$f(\omega t) = \sum_{n=1,3,5,7\ldots} \frac{4V_{dc}}{n\pi}\left[1 + 2\sum_{r=1}^{N}(-1)^r \cos(n\alpha_r)\right]\sin(n\omega t)$$

2.2.3 Single phase unipolar scheme

The PWM output voltage waveform has 3 switching levels, $+V_{dc}$, 0 and $-V_{dc}$. The waveform has either of the values $+V_{dc}$ or 0 during the positive half cycle of the ideal reference sinusoidal waveform, and either of the values $-V_{dc}$ or 0 during the negative half cycle of the ideal reference sinusoidal waveform. The gating signals for the switches in the two inverter legs must be generated separately. The nature of the output voltage waveform for odd and even number of switching angles per quarter cycle is given in Figure 2.7 and Figure 2.8 respectively.

The Fourier series expansion of the output voltage waveform is given below.

$$f(\omega t) = \sum_{n=1,3,5,7\ldots} \frac{4V_{dc}}{n\pi}\left[\sum_{r=1}^{N}(-1)^{r+1} \cos(n\alpha_r)\right]\sin(n\omega t)$$

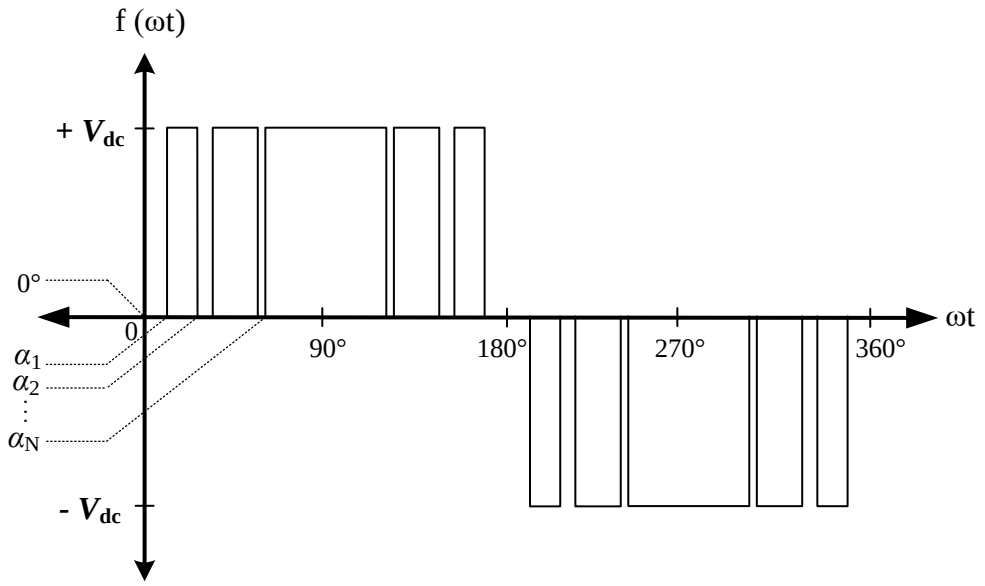

Figure 2.7. PWM output voltage waveform for unipolar scheme in the full-bridge inverter (odd number of switching angles per quarter cycle)

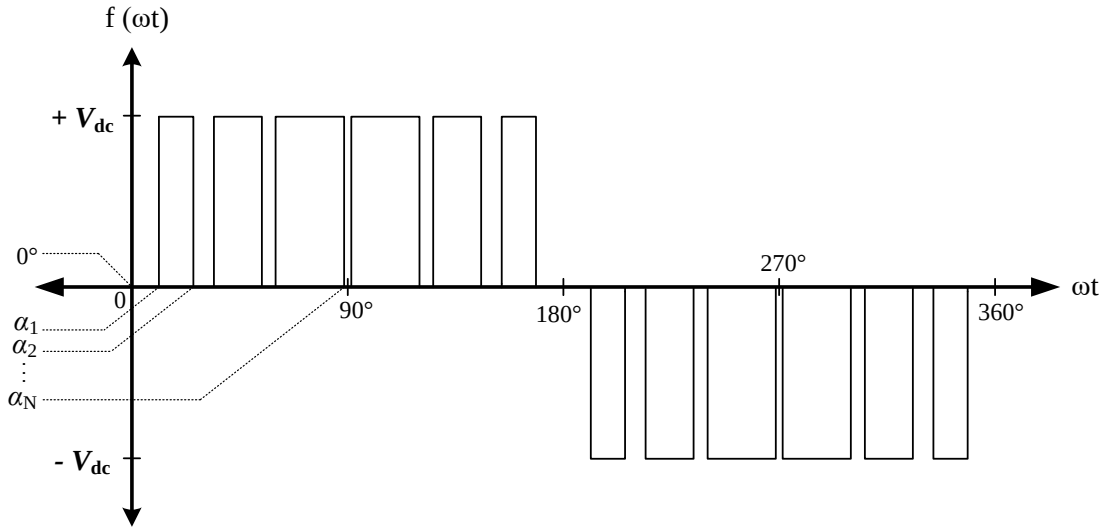

Figure 2.8. PWM output voltage waveform for unipolar scheme in the full-bridge inverter (even number of switching angles per quarter cycle)

2.3 PWM SCHEMES FOR THE THREE-PHASE INVERTER

The three-phase inverter configuration is given in Figure 2.9. The PWM output line-to-line voltage waveform has 3 switching levels, $+V_{dc}$, 0 and $-V_{dc}$. The gating signals for the switches in the three inverter legs are symmetrical and shifted 120° apart from each other. Therefore, each of the triplen harmonic components have equal magnitudes and phase in the three phase voltage waveforms, and are absent in the line-to-line voltage waveforms obtained as the difference of two phase voltage waveforms.

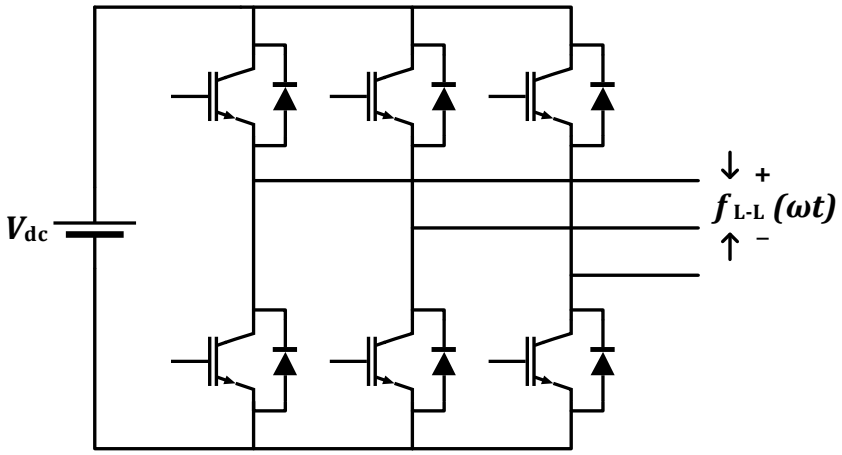

Fig. 2.9. Three-phase inverter configuration

The PWM output phase voltage waveforms have two switching levels, $+\frac{V_{dc}}{2}$ and $-\frac{V_{dc}}{2}$. Each phase leg of the three-phase inverter behaves as a half-bridge inverter itself. The values of the switching angles are determined to eliminate the low order odd harmonics except triplen harmonics, i.e. the 5th, 7th, 11th, 13th… harmonics are eliminated in the output phase voltage waveform. $f_{phase}(\omega t)$ denotes the output phase voltage.

2.3.1 Three phase scheme A

The PWM output phase voltage waveform representing one sinusoidal cycle begins with a magnitude of $-\frac{V_{dc}}{2}$ at phase 0°. This is the same scheme as the bipolar PWM scheme A employed in half-bridge inverters.

The Fourier series expansion of the output voltage waveforms is given below.

$$f_{phase}(\omega t) = \sum_{n=1,3,5,7\ldots} -\frac{2V_{dc}}{n\pi}\left[1 + 2\sum_{r=1}^{N}(-1)^r \cos(n\alpha_r)\right]\sin(n\omega t)$$

$$f_{L-L}(\omega t) = \sum_{n=1,5,7,11\ldots} (-1)^{(n \bmod 3)}\frac{2\sqrt{3}V_{dc}}{n\pi}\left[1 + 2\sum_{r=1}^{N}(-1)^r \cos(n\alpha_r)\right]\sin(n\omega t)$$

2.3.2 Three phase scheme B

The PWM output phase voltage waveform representing one sinusoidal cycle begins with a magnitude of $+\frac{V_{dc}}{2}$ at phase 0°. This is the same scheme as the bipolar PWM scheme B employed in half-bridge inverters.

The Fourier series expansion of the output voltage waveforms is given below.

$$f_{phase}(\omega t) = \sum_{n=1,3,5,7\ldots} \frac{2V_{dc}}{n\pi}\left[1 + 2\sum_{r=1}^{N}(-1)^r \cos(n\alpha_r)\right]\sin(n\omega t)$$

$$f_{L-L}(\omega t) = \sum_{n=1,5,7,11\ldots} (-1)^{1+(n \bmod 3)}\frac{2\sqrt{3}V_{dc}}{n\pi}\left[1 + 2\sum_{r=1}^{N}(-1)^r \cos(n\alpha_r)\right]\sin(n\omega t)$$

2.4 SUMMARY

The classification of the various programmed PWM schemes is discussed. The nature of the output PWM voltage waveforms produced by various PWM schemes for the half-bridge, full-bridge and three-phase inverters is analysed in detail and the Fourier series expansion of the output voltage waveforms is discussed. The details of the harmonics required to be eliminated for the different PWM schemes is discussed.

CHAPTER 3

SOLVING FOR THE SWITCHING ANGLES FOR SELECTIVE HARMONIC ELIMINATION IN PROGRAMMED PWM SCHEMES

The Fourier series expansion of the output pulsewidth modulated voltage waveforms generated using programmed PWM techniques are discussed in Chapter 2. In the present chapter, the focus is on solving for the switching angles such that SHE is achieved. If the number of harmonics to be eliminated is N-1, the problem is essentially that of solving N simultaneous nonlinear equations – N-1 equations associated with eliminating the undesired harmonics, and one equation specifying the magnitude of the fundamental component of the output voltage waveform.

The conventional gradient-based optimization algorithms such as the conjugate gradient, Newton-Raphson and Gauss-Seidel methods that are used for solving nonlinear simultaneous equations may not necessarily converge at the solutions of this problem. The solutions arrived at by the gradient-based algorithms are largely dependent upon the starting point of the algorithm and are very likely to converge at a local optimum solution rather than the required global optimum solution. Alternative optimization algorithms that have theoretically been proved to be capable of reaching the global optimum solutions of systems of simultaneous nonlinear equations are the class of evolutionary algorithms.

The evolutionary algorithms [7] are based on principles inspired from the genetic and evolution mechanisms observed in natural systems. These algorithms are stochastic in nature, contrary to the deterministic gradient-based algorithms. The three major classes of evolutionary algorithms are the genetic algorithm, genetic programming, and evolutionary programming. In this work, we employ the genetic algorithm [8], [9] to determine the optimum switching angles of the programmed PWM schemes discussed.

3.1 THE GENETIC ALGORITHM

3.1.1 Representation and Initialization

The first step in defining the genetic algorithm is to link the original problem context to the problem-solving space where genetic evolution takes place. Objects forming possible solutions within the original problem context are called phenotypes. In the programmed PWM problem under consideration, all combinations of N switching angles within the $\left(0, {}^{\pi}/_{2}\right)$ interval, not necessarily resulting in SHE in the output PWM voltage waveform, constitute phenotypes. The phenotypes are encoded as individuals or chromosomes within the genetic algorithm space, called genotypes. While a phenotype may have many genotype representations, each genotype maps back to one and only one phenotype. A set of N switching angles $(\alpha_1, \alpha_2 \ldots \alpha_N)$ that constitute a phenotype are represented as a binary encoded string in the GA genotype space. The substrings of the chromosome constitute the representation of the individual switching angles $\alpha_1, \alpha_2 \ldots \alpha_N$ in the GA space. Each bit in the chromosome binary string in the GA space is referred to as a gene.

Once the representation is specified, the initial population of genotypes is seeded by randomly generated individuals.

3.1.2 Fitness Evaluation

The quality of the genotypes in the generated population is assessed by evaluating the fitness of each of the genotypes using a fitness function. The original optimization problem was to determine the phenotype that minimizes a given objective function. The fitness function is essentially transformation of the objective function that takes arguments from the GA space, i.e. genotypes as input. The genotypes corresponding to phenotypes having low objective function values have high fitness. The role of the fitness function is to represent the requirements that the population must adapt to meet. It forms the basis for selection, and so, facilitates improvements.

3.1.3 Parent Selection

The role of parent selection is to distinguish among individuals based on their quality, and to allow the better individuals to become parents of the next generation. Chromosomes from the population are selected in pairs with a probability proportional to their fitness. The selected chromosomes are duplicated (reproduced) to be used in the production of offspring. Thus, high quality chromosomes have more chance of becoming parents than those with low quality. Nevertheless, low-quality individuals are often given a small, but positive chance; otherwise the whole search could become too greedy and the population could get stuck in a local optimum.

3.1.4 Recombination

Recombination is the primary variation operator in the genetic algorithm. In accordance with the crossover rate, randomly chosen pairs of parent chromosomes from the population produced after duplication undergo crossover or recombination to produce offspring. The recombination operator merges information from two parent chromosomes into two offspring chromosomes. The principle behind recombination is this – by mating two individuals with different but desirable features, offspring that combine features from both the parents can be produced. While some offspring will have undesirable combination of traits from parents, and most may be no better or worse than their parents, some will have improved characteristics. In the binary string representation of phenotypes in the GA space in the present problem, recombination constitutes the selection of a random cut point in the parent chromosomes and the exchange of the substrings of the parent strings beyond the cut point.

3.1.5 Mutation

Mutation is a unary variation operator that operates on individual chromosomes in the population. In accordance with the mutation rate, some chromosomes from the population produced after crossover are randomly selected for mutation. These chromosomes are altered to deliver slightly modified mutant chromosomes. In the binary string representation of phenotypes in the GA space in the present problem, mutation constitutes the inversion of random bits (genes) in the parent chromosomes (bit sequences) selected for mutation.

Variation operators such as the recombination and mutation operators in the genetic algorithm constitute the implementation of elementary search steps, giving the search space its topological structure. Generating a child amounts to stepping a new point in this space. From this perspective, mutation guarantees that the space is connected. The connectedness property of the space ensures that each genotype representing a possible solution can be reached by the variation operators.

3.1.6 Survivor Selection

The individuals in the population created after mutation are ranked in order of their fitness. The individuals with the highest quality qualify to proceed to the next generation. Once the next generation of population is thus created, the steps 2 – 6 are repeated till an individual with the desired maximum fitness is created.

3.2 EXPERIMENTAL RESULTS

The optimized switching angles for the different programmed PWM schemes are solved for using the genetic algorithm. The trend followed by the switching angles with respect to the modulation index *M* is observed. The modulation index *M* is the ratio of the peak-to-peak magnitude of the fundamental component of the output PWM voltage waveform and the absolute peak-to-peak magnitude of the output PWM voltage waveform.

3.2.1 Single phase inverters

3.2.1.1 Bipolar PWM Scheme A

3.2.1.1.1 Odd number of switching angles per quarter cycle

The number of switching angles per quarter cycle is fixed at N = 5. The 3^{rd}, 5^{th}, 7^{th}, and 9^{th} harmonic components in the output voltage waveform are selectively eliminated. The equations that are solved to determine the switching angles α_1, α_2, α_3, α_4, α_5 are given below.

$$\frac{4}{\pi}(-1+2\cos\alpha_1-2\cos\alpha_2+2\cos\alpha_3-2\cos\alpha_4+2\cos\alpha_5)-M=0$$

$$\frac{4}{3\pi}(-1+2\cos(3\alpha_1)-2\cos(3\alpha_2)+2\cos(3\alpha_3)-2\cos(3\alpha_4)+2\cos(3\alpha_5))=0$$

$$\frac{4}{5\pi}(-1+2\cos(5\alpha_1)-2\cos(5\alpha_2)+2\cos(5\alpha_3)-2\cos(5\alpha_4)+2\cos(5\alpha_5))=0$$

$$\frac{4}{7\pi}(-1+2\cos(7\alpha_1)-2\cos(7\alpha_2)+2\cos(7\alpha_3)-2\cos(7\alpha_4)+2\cos(7\alpha_5))=0$$

$$\frac{4}{9\pi}(-1+2\cos(9\alpha_1)-2\cos(9\alpha_2)+2\cos(9\alpha_3)-2\cos(9\alpha_4)+2\cos(9\alpha_5))=0$$

The values of the switching angles obtained by optimization using the genetic algorithm are given in Table 3.1. A plot of the magnitude of the optimized switching angles versus the modulation index *M* is given in Figure 3.1.

3.2.1.1.1 Even number of switching angles per quarter cycle

The number of switching angles per quarter cycle is fixed at N = 4. The 3rd, 5th and 7th harmonic components in output voltage waveform are selectively eliminated. The equations that are solved to determine the switching angles α_1, α_2, α_3, α_4 are given below.

$$\frac{4}{\pi}(-1+2\cos\alpha_1-2\cos\alpha_2+2\cos\alpha_3-2\cos\alpha_4+2\cos\alpha_5)-M=0$$

$$\frac{4}{3\pi}(-1+2\cos(3\alpha_1)-2\cos(3\alpha_2)+2\cos(3\alpha_3)-2\cos(3\alpha_4))=0$$

$$\frac{4}{5\pi}(-1+2\cos(5\alpha_1)-2\cos(5\alpha_2)+2\cos(5\alpha_3)-2\cos(5\alpha_4))=0$$

$$\frac{4}{7\pi}(-1+2\cos(7\alpha_1)-2\cos(7\alpha_2)+2\cos(7\alpha_3)-2\cos(7\alpha_4))=0$$

The values of the switching angles obtained by optimization using the genetic algorithm are given in Table 3.2. A plot of the magnitude of the optimized switching angles versus the modulation index *M* is given in Figure 3.2.

M \ α	α_1	α_2	α_3	α_4	α_5
0.0	16.3636°	32.7273°	49.0909°	65.4545°	81.8182°
0.1	16.1193°	33.1451°	48.4466°	66.1792°	81.0001°
0.2	15.8486°	33.5108°	47.7495°	66.8643°	80.1615°
0.3	15.5528°	33.8175°	46.9958°	67.5070°	79.2946°
0.4	15.2325°	34.0551°	46.1779°	68.0990°	78.3874°
0.5	14.8872°	34.2081°	45.2834°	68.6241°	77.4201°
0.6	14.5147°	34.2531°	44.2920°	69.0495°	76.3573°
0.7	14.1100°	34.1520°	43.1700°	69.3046°	75.1266°
0.8	13.6612°	33.8362°	41.8552°	69.2092°	73.5484°
0.9	13.1320°	33.1408°	40.1917°	68.1320°	71.0048°
1.0	12.1705°	30.7697°	36.8753°	60.9825°	62.6427°

Table 3.1. Optimized switching angles for bipolar PWM scheme A in the single-phase inverter (odd number of switching angles per quarter cycle)

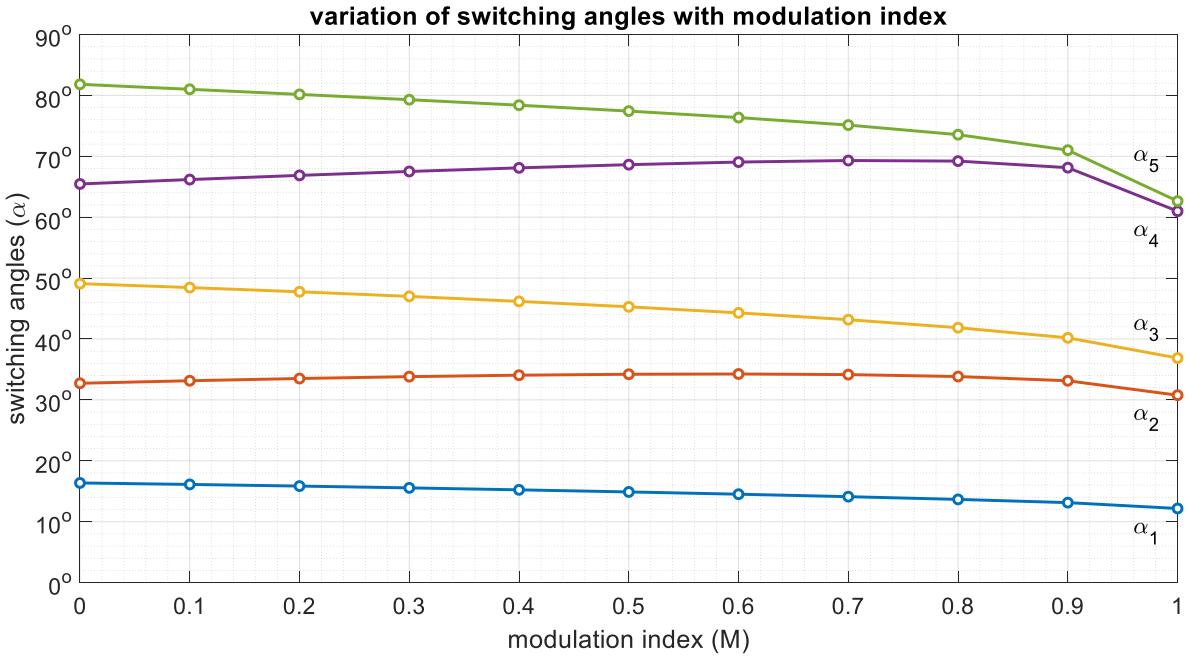

Figure 3.1. Optimized switching angles versus modulation index for bipolar PWM scheme A in the single-phase inverter (odd number of switching angles per quarter cycle)

α / M	α_1	α_2	α_3	α_4
0.0	20.0000°	40.0000°	60.0000°	80.0000°
0.1	19.6390°	40.6120°	59.1071°	80.9754°
0.2	19.2421°	41.1582°	58.1573°	81.9355°
0.3	18.8118°	41.6291°	57.1425°	82.8849°
0.4	18.3492°	42.0093°	56.0488°	83.8273°
0.5	17.8541°	42.2746°	54.8543°	84.7663°
0.6	17.3240°	42.3860°	53.5235°	85.7051°
0.7	16.7528°	42.2790°	51.9980°	86.6475°
0.8	16.1266°	41.8388°	50.1749°	87.5979°
0.9	15.4123°	40.8421°	47.8562°	88.5624°
1.0	14.5135°	38.7859°	44.6065°	89.5506°

Table 3.2. Optimized switching angles for bipolar PWM scheme A in the single-phase inverter (even number of switching angles per quarter cycle)

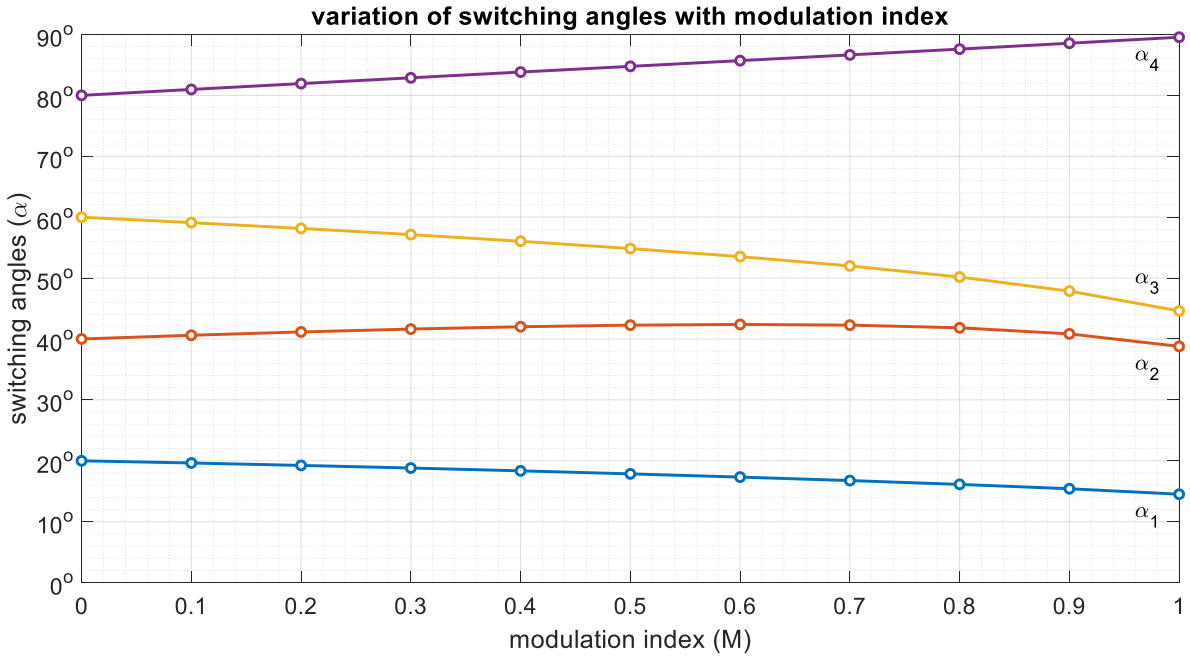

Figure 3.2. Optimized switching angles versus modulation index for bipolar PWM scheme A in the single-phase inverter (even number of switching angles per quarter cycle)

3.2.1.2 Bipolar PWM Scheme B

3.2.1.2.1 Odd number of switching angles per quarter cycle

The number of switching angles per quarter cycle is fixed at N = 5. The 3rd, 5th, 7th and 9th harmonic components in the output voltage waveform are selectively eliminated. The equations that are solved to determine the switching angles α_1, α_2, α_3, α_4, α_5 are given below.

$$\frac{4}{\pi}(1 - 2\cos\alpha_1 + 2\cos\alpha_2 - 2\cos\alpha_3 + 2\cos\alpha_4 - 2\cos\alpha_5) - M = 0$$

$$\frac{4}{3\pi}(1 - 2\cos(3\alpha_1) + 2\cos(3\alpha_2) - 2\cos(3\alpha_3) + 2\cos(3\alpha_4) - 2\cos(3\alpha_5)) = 0$$

$$\frac{4}{5\pi}(1 - 2\cos(5\alpha_1) + 2\cos(5\alpha_2) - 2\cos(5\alpha_3) + 2\cos(5\alpha_4) - 2\cos(5\alpha_5)) = 0$$

$$\frac{4}{7\pi}(1 - 2\cos(7\alpha_1) + 2\cos(7\alpha_2) - 2\cos(7\alpha_3) + 2\cos(7\alpha_4) - 2\cos(7\alpha_5)) = 0$$

$$\frac{4}{9\pi}(1 - 2\cos(9\alpha_1) + 2\cos(9\alpha_2) - 2\cos(9\alpha_3) + 2\cos(9\alpha_4) - 2\cos(9\alpha_5)) = 0$$

The values of the switching angles obtained by optimization using the genetic algorithm are given in Table 3.3. A plot of the magnitude of the optimized switching angles versus the modulation index *M* is given in Figure 3.3.

3.2.1.2.2 Even number of switching angles per quarter cycle

The number of switching angles per quarter cycle is fixed at N = 6. The 3rd, 5th, 7th, 9th and 11th harmonic components in output voltage waveform are selectively eliminated. The equations that are solved to determine the switching angles α_1, α_2, α_3, α_4, α_5, α_6 are given below.

$$\frac{4}{\pi}(1 - 2\cos\alpha_1 + 2\cos\alpha_2 - 2\cos\alpha_3 + 2\cos\alpha_4 - 2\cos\alpha_5 + 2\cos\alpha_6) - M = 0$$

$$\frac{4}{3\pi}(1 - 2\cos(3\alpha_1) + 2\cos(3\alpha_2) - 2\cos(3\alpha_3) + 2\cos(3\alpha_4) - 2\cos(3\alpha_5) + 2\cos(3\alpha_6)) = 0$$

$$\frac{4}{5\pi}(1 - 2\cos(5\alpha_1) + 2\cos(5\alpha_2) - 2\cos(5\alpha_3) + 2\cos(5\alpha_4) - 2\cos(5\alpha_5) + 2\cos(5\alpha_6)) = 0$$

α / M	α_1	α_2	α_3	α_4	α_5
0.0	16.3636°	32.7273°	49.0909°	65.4545°	81.8182°
0.1	16.5795°	32.2614°	49.6829°	64.6899°	82.6214°
0.2	16.7639°	31.7497°	50.2197°	63.8814°	83.4137°
0.3	16.9131°	31.1922°	50.6945°	63.0213°	84.1985°
0.4	17.0219°	30.5871°	51.0946°	62.0966°	84.9786°
0.5	17.0832°	29.9302°	51.3984°	61.0861°	85.7563°
0.6	17.0874°	29.2136°	51.5686°	59.9539°	86.5344°
0.7	17.0191°	28.4231°	51.5378°	58.6362°	87.3157°
0.8	16.8518°	27.5307°	51.1716°	57.0078°	88.1042°
0.9	16.5272°	26.4694°	50.1632°	54.7857°	88.9060°
1.0	15.8539°	25.0060°	47.6222°	51.1659°	89.7333°

Table 3.3. Optimized switching angles for bipolar PWM scheme B in the single-phase inverter (odd number of switching angles per quarter cycle)

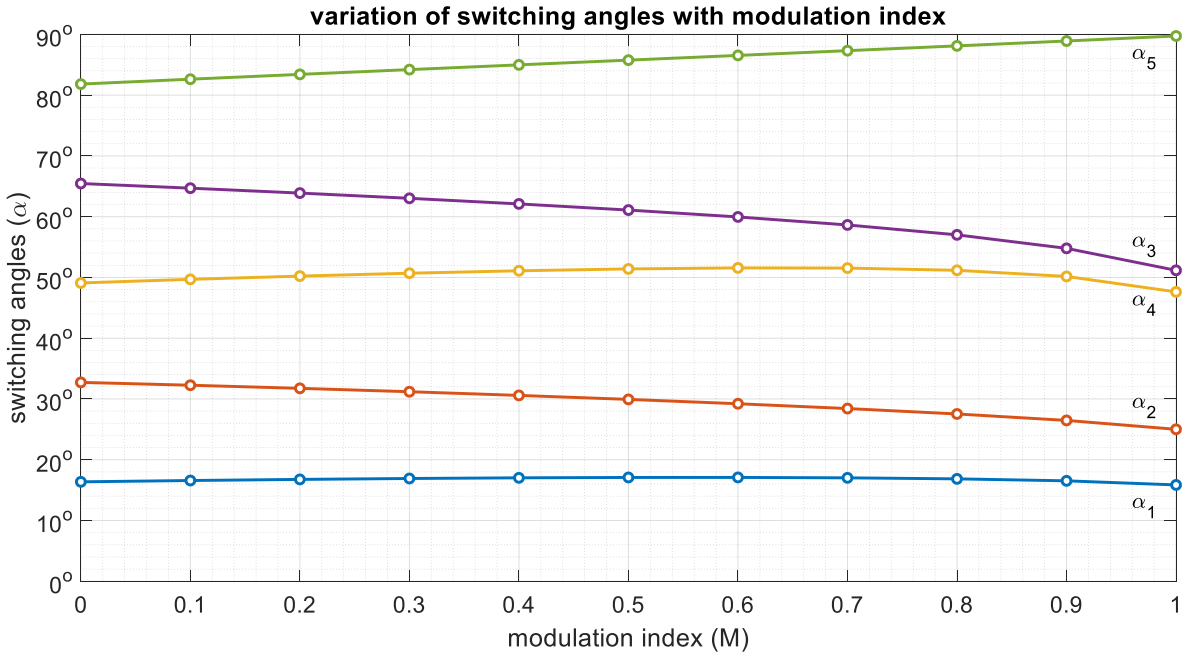

Figure 3.3. Optimized switching angles versus modulation index for bipolar PWM scheme B in the single-phase inverter (odd number of switching angles per quarter cycle)

$$\frac{4}{7\pi}(1 - 2\cos(7\alpha_1) + 2\cos(7\alpha_2) - 2\cos(7\alpha_3) + 2\cos(7\alpha_4) - 2\cos(7\alpha_5) + 2\cos(7\alpha_6)) = 0$$

$$\frac{4}{9\pi}(1 - 2\cos(9\alpha_1) + 2\cos(9\alpha_2) - 2\cos(9\alpha_3) + 2\cos(9\alpha_4) - 2\cos(9\alpha_5) + 2\cos(9\alpha_6)) = 0$$

$$\frac{4}{11\pi}(1 - 2\cos(11\alpha_1) + 2\cos(11\alpha_2) - 2\cos(11\alpha_3) + 2\cos(11\alpha_4) - 2\cos(11\alpha_5) + 2\cos(11\alpha_6)) = 0$$

The values of the switching angles obtained by optimization using the genetic algorithm are given in Table 3.4. A plot of the magnitude of the optimized switching angles versus the modulation index *M* is given in Figure 3.4.

3.2.1.3 Unipolar PWM Scheme (only in full-bridge inverter)

3.2.1.3.1 Odd number of switching angles per quarter cycle

The number of switching angles per quarter cycle is fixed at N = 5. The 3rd, 5th, 7th and 9th harmonic components in the output voltage waveform are selectively eliminated. The equations that are solved to determine the switching angles α_1, α_2, α_3, α_4, α_5 are given below.

$$\frac{4}{\pi}(\cos\alpha_1 - \cos\alpha_2 + \cos\alpha_3 - \cos\alpha_4 + \cos\alpha_5) - M = 0$$

$$\frac{4}{3\pi}(\cos(3\alpha_1) - \cos(3\alpha_2) + \cos(3\alpha_3) - \cos(3\alpha_4) + \cos(3\alpha_5)) = 0$$

$$\frac{4}{5\pi}(\cos(5\alpha_1) - \cos(5\alpha_2) + \cos(5\alpha_3) - \cos(5\alpha_4) + 5\cos(5\alpha_5)) = 0$$

$$\frac{4}{7\pi}(\cos(7\alpha_1) - \cos(7\alpha_2) + \cos(7\alpha_3) - \cos(7\alpha_4) + \cos(7\alpha_5)) = 0$$

$$\frac{4}{9\pi}(\cos(9\alpha_1) - \cos(9\alpha_2) + \cos(9\alpha_3) - \cos(9\alpha_4) + \cos(9\alpha_5)) = 0$$

The values of the switching angles obtained by optimization using the genetic algorithm are given in Table 3.5. A plot of the magnitude of the optimized switching angles versus the modulation index *M* is given in Figure 3.5.

M \ α	α_1	α_2	α_3	α_4	α_5	α_6
0.0	13.8462°	27.6923°	41.5385°	55.3846°	69.2308°	83.0769°
0.1	14.0009°	27.3520°	41.9743°	54.7932°	69.8631°	82.3835°
0.2	14.1322°	26.9753°	42.3614°	54.1570°	70.4655°	81.6750°
0.3	14.2378°	26.5625°	42.6938°	53.4711°	71.0362°	80.9453°
0.4	14.3140°	26.1126°	42.9615°	52.7269°	71.5696°	80.1858°
0.5	14.3564°	25.6226°	43.1487°	51.9099°	72.0539°	79.3818°
0.6	14.3581°	25.0869°	43.2294°	50.9963°	72.4653°	78.5070°
0.7	14.3088°	24.4950°	43.1592°	49.9455°	72.7514°	77.5066°
0.8	14.1894°	23.8255°	42.8543°	48.6803°	72.7745°	76.2416°
0.9	13.9529°	23.0198°	42.1150°	47.0152°	72.0192°	74.2020°
1.0	12.0982°	19.9634°	35.9638°	40.0195°	58.7866°	60.1040°

Table 3.4. Optimized switching angles for bipolar PWM scheme B in the single-phase inverter (even number of switching angles per quarter cycle)

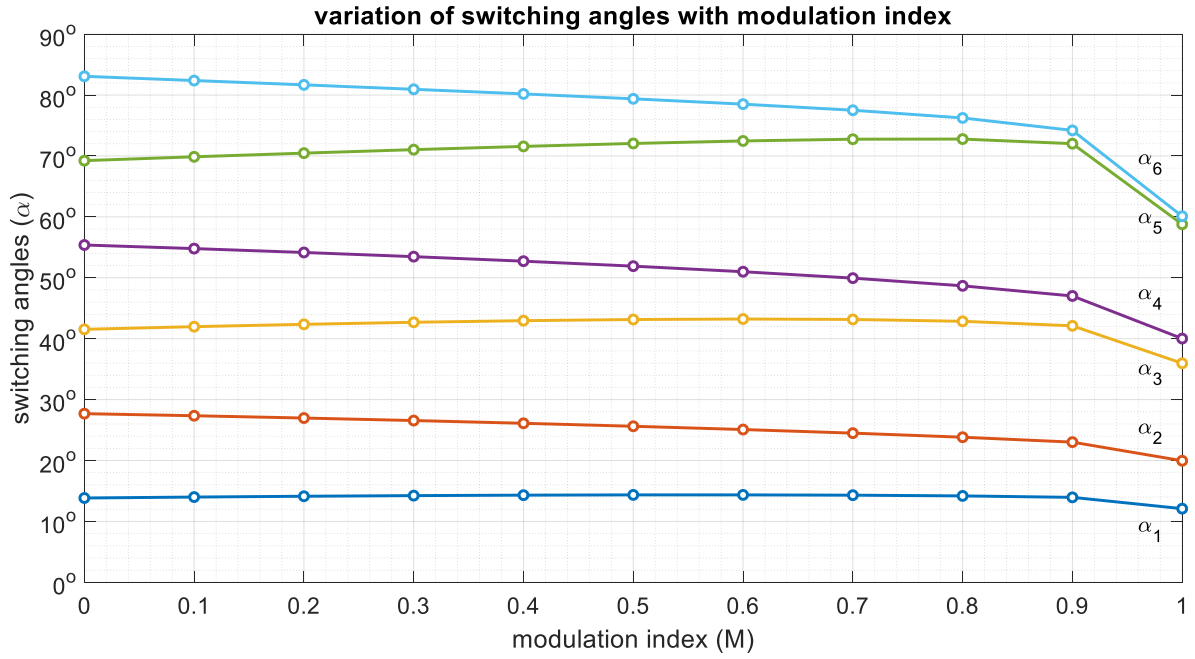

Figure 3.4. Optimized switching angles versus modulation index for bipolar PWM scheme B in the single-phase inverter (even number of switching angles per quarter cycle)

α / **M**	α_1	α_2	α_3	α_4	α_5
0.0	30.0000°	30.0000°	60.0000°	60.0000°	90.0000°
0.1	29.2343°	30.7323°	58.6836°	61.2824°	88.4985°
0.2	28.4385°	31.4228°	57.3295°	62.5310°	86.9873°
0.3	27.6172°	32.0631°	55.9321°	63.7437°	85.4557°
0.4	26.7718°	32.6396°	54.4818°	64.9137°	83.8892°
0.5	25.9023°	33.1333°	52.9645°	66.0266°	82.2666°
0.6	25.0067°	33.5160°	51.3586°	67.0530°	80.5523°
0.7	24.0785°	33.7436°	49.6289°	67.9281°	78.6760°
0.8	23.1019°	33.7381°	47.7118°	68.4834°	76.4669°
0.9	22.0274°	33.3203°	45.4513°	68.1122°	73.3370°
1.0	20.3463°	31.1306°	41.5105°	61.5229°	64.4216°

Table 3.5. Optimized switching angles for unipolar PWM scheme in the single-phase full-bridge inverter (odd number of switching angles per quarter cycle)

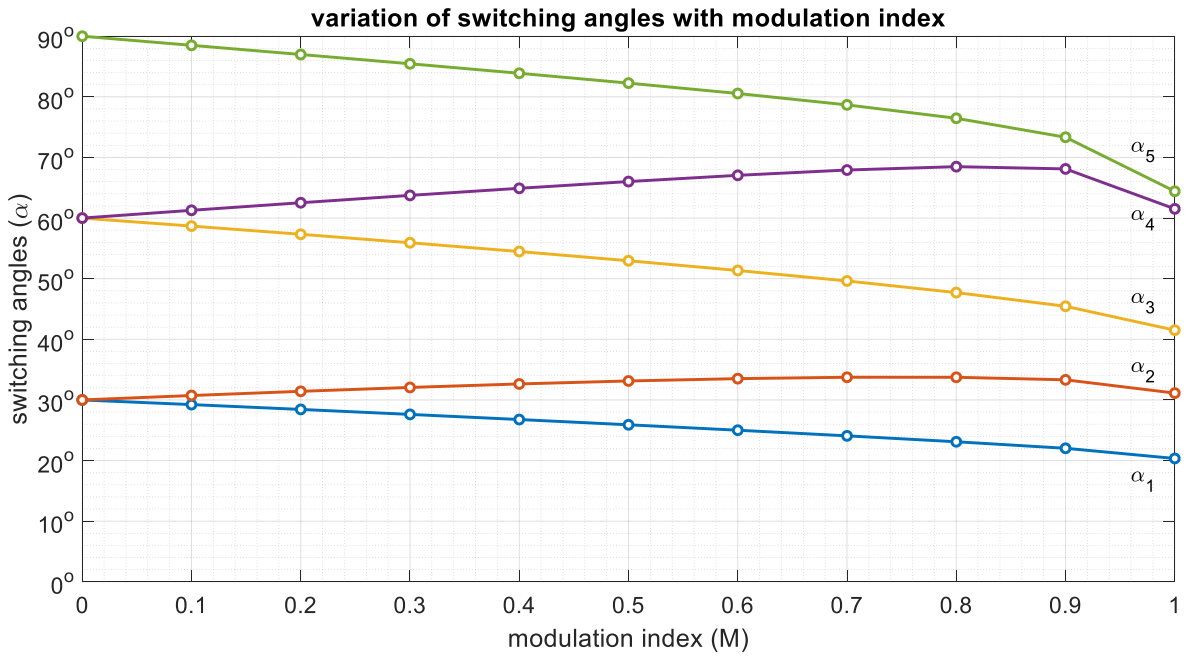

Figure 3.5. Optimized switching angles versus modulation index for unipolar PWM scheme in the single-phase full-bridge inverter (odd number of switching angles per quarter cycle)

3.2.1.3.2 Even number of switching angles per quarter cycle

The number of switching angles per quarter cycle is fixed at N = 4. The 3rd, 5th and 7th harmonic components in the output voltage waveform are selectively eliminated. The equations that are solved to determine the switching angles α_1, α_2, α_3, α_4 are given below.

$$\frac{4}{\pi}(\cos\alpha_1 - \cos\alpha_2 + \cos\alpha_3 - \cos\alpha_4) - M = 0$$

$$\frac{4}{3\pi}(\cos(3\alpha_1) - \cos(3\alpha_2) + \cos(3\alpha_3) - \cos(3\alpha_4)) = 0$$

$$\frac{4}{5\pi}(\cos(5\alpha_1) - \cos(5\alpha_2) + \cos(5\alpha_3) - \cos(5\alpha_4)) = 0$$

$$\frac{4}{7\pi}(\cos(7\alpha_1) - \cos(7\alpha_2) + \cos(7\alpha_3) - \cos(7\alpha_4)) = 0$$

The values of the switching angles obtained by optimization using the genetic algorithm are given in Table 3.6. A plot of the magnitude of the optimized switching angles versus the modulation index *M* is given in Figure 3.6.

$\boldsymbol{\alpha}$ / **M**	$\boldsymbol{\alpha_1}$	$\boldsymbol{\alpha_2}$	$\boldsymbol{\alpha_3}$	$\boldsymbol{\alpha_4}$
0.0	36.0000°	36.0000°	72.0000°	72.0000°
0.1	34.9255°	37.0391°	70.2756°	73.7022°
0.2	33.8202°	38.0330°	68.5193°	75.3898°
0.3	32.6886°	38.9698°	66.7186°	77.0695°
0.4	31.5326°	39.8313°	64.8568°	78.7477°
0.5	30.3521°	40.5895°	62.9093°	80.4303°
0.6	29.1439°	41.2010°	60.8387°	82.1241°
0.7	27.9003°	41.5931°	58.5840°	83.8372°
0.8	26.6026°	41.6352°	56.0378°	85.5798°
0.9	25.2042°	41.0650°	52.9894°	87.3672°
1.0	23.5598°	39.2595°	48.9600°	89.2240°

Table 3.6. Optimized switching angles for unipolar PWM scheme in the single-phase full-bridge inverter (even number of switching angles per quarter cycle)

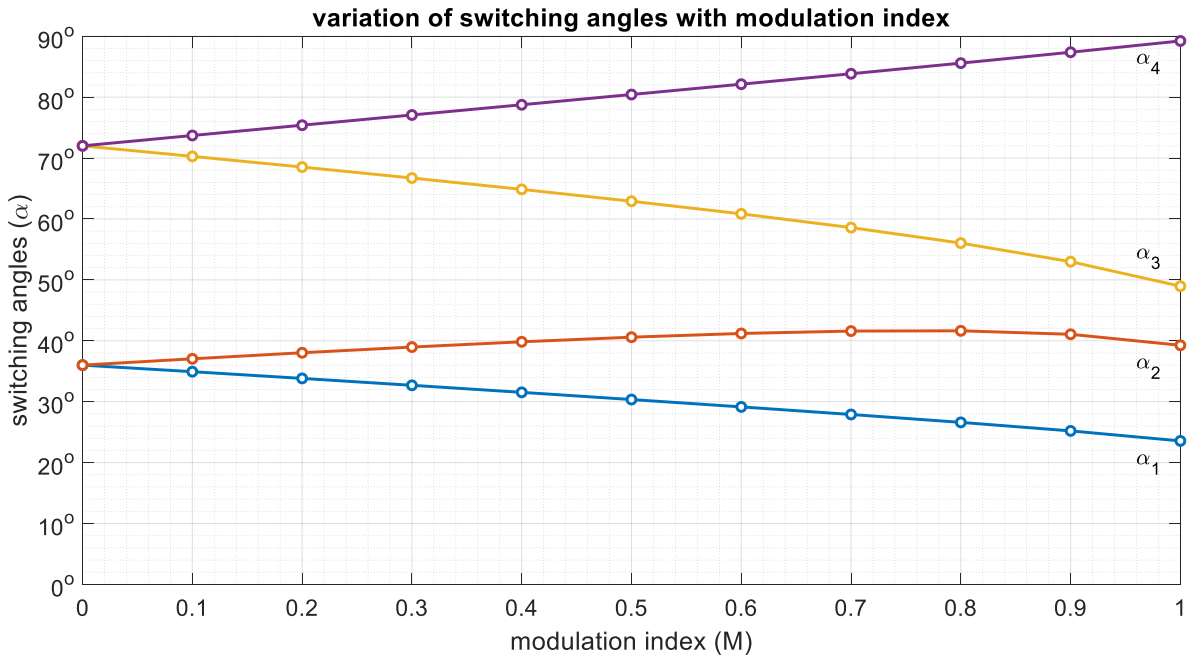

Figure 3.6. Optimized switching angles versus modulation index for unipolar PWM scheme in the single-phase full-bridge inverter (even number of switching angles per quarter cycle)

3.2.2 Three phase inverters

3.2.2.1 Scheme A

The number of switching angles per quarter cycle is fixed at N = 5. The 5^{th}, 7^{th}, 11^{th}, and 13^{th} harmonic components in the output phase voltage waveform are selectively eliminated. The equations that are solved to determine the switching angles α_1, α_2, α_3, α_4, α_5 are given below.

$$\frac{4}{\pi}(-1 + 2\cos\alpha_1 - 2\cos\alpha_2 + 2\cos\alpha_3 - 2\cos\alpha_4 + 2\cos\alpha_5) - M = 0$$

$$\frac{4}{5\pi}(-1 + 2\cos(5\alpha_1) - 2\cos(5\alpha_2) + 2\cos(5\alpha_3) - 2\cos(5\alpha_4) + 2\cos(5\alpha_5)) = 0$$

$$\frac{4}{7\pi}(-1 + 2\cos(7\alpha_1) - 2\cos(7\alpha_2) + 2\cos(7\alpha_3) - 2\cos(7\alpha_4) + 2\cos(7\alpha_5)) = 0$$

$$\frac{4}{11\pi}(-1 + 2\cos(11\alpha_1) - 2\cos(11\alpha_2) + 2\cos(11\alpha_3) - 2\cos(11\alpha_4) + 2\cos(11\alpha_5)) = 0$$

$$\frac{4}{13\pi}(-1 + 2\cos(13\alpha_1) - 2\cos(13\alpha_2) + 2\cos(13\alpha_3) - 2\cos(13\alpha_4) + 2\cos(13\alpha_5)) = 0$$

The values of the switching angles obtained by optimization using the genetic algorithm are given in Table 3.7. A plot of the magnitude of the optimized switching angles versus the modulation index *M* is given in Figure 3.7.

3.2.2.1 Scheme B

The number of switching angles per quarter cycle is fixed at N = 4. The 5^{th}, 7^{th} and 11^{th} harmonic components in the output phase voltage waveform are selectively eliminated. The equations that are solved to determine the switching angles $\alpha_1, \alpha_2, \alpha_3, \alpha_4$ are given below.

$$\frac{4}{\pi}(1 - 2\cos\alpha_1 + 2\cos\alpha_2 - 2\cos\alpha_3 + 2\cos\alpha_4) - M = 0$$

$$\frac{4}{5\pi}(1 - 2\cos(5\alpha_1) + 2\cos(5\alpha_2) - 2\cos(5\alpha_3) + 2\cos(5\alpha_4)) = 0$$

$$\frac{4}{7\pi}(1 - 2\cos(7\alpha_1) + 2\cos(7\alpha_2) - 2\cos(7\alpha_3) + 2\cos(7\alpha_4)) = 0$$

$$\frac{4}{11\pi}(1 - 2\cos(11\alpha_1) + 2\cos(11\alpha_2) - 2\cos(11\alpha_3) + 2\cos(11\alpha_4)) = 0$$

The values of the switching angles obtained by optimization using the genetic algorithm are given in Table 3.8. A plot of the magnitude of the optimized switching angles versus the modulation index *M* is given in Figure 3.8.

3.3 COMPARISON BETWEEN OPTIMIZATION ALGORITHMS

Here, we compare between the implementation of the genetic algorithm and the sequential quadratic programming algorithm, a conventional gradient-based algorithm to solve the problem of selective harmonic elimination in PWM inverters. The comparison is presented in Table 3.9. *N* denotes the number of switching angles per quarter cycle.

α / M	α_1	α_2	α_3	α_4	α_5
0.0	20.0000°	20.0000°	40.0000°	40.0000°	60.0000°
0.1	19.1215°	20.4537°	39.0881°	40.7230°	59.1299°
0.2	18.2316°	20.9054°	38.1603°	41.4458°	58.2504°
0.3	17.3289°	21.3507°	37.2133°	42.1671°	57.3593°
0.4	16.4117°	21.7843°	36.2426°	42.8846°	56.4533°
0.5	15.4779°	22.1986°	35.2418°	43.5950°	55.5281°
0.6	14.5241°	22.5826°	34.2010°	44.2928°	54.5766°
0.7	13.5462°	22.9190°	33.1048°	44.9674°	53.5871°
0.8	12.5371°	23.1789°	31.9273°	45.5983°	52.5370°
0.9	11.4855°	23.3086°	30.6199°	46.1367°	51.3753°
1.0	10.3669°	23.1920°	29.0769°	46.4319°	49.9495°

Table 3.7. Optimized switching angles for bipolar PWM scheme A in the three-phase inverter (odd number of switching angles per quarter cycle)

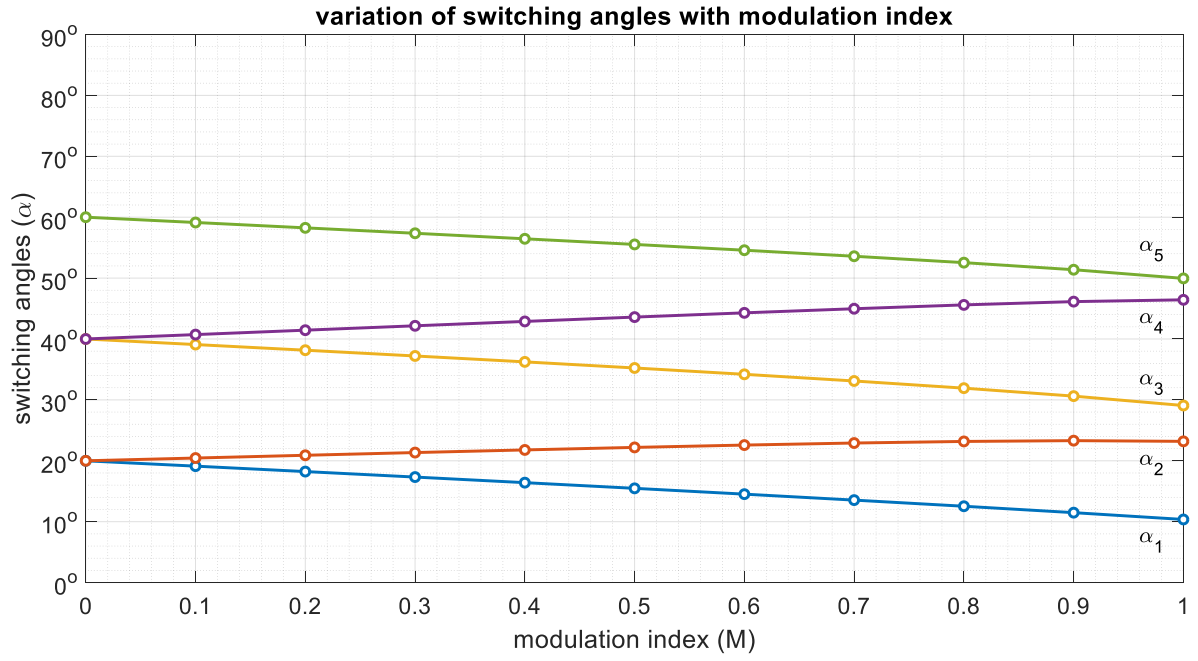

Figure 3.7. Optimized switching angles versus modulation index for PWM scheme A in the three-phase inverter (odd number of switching angles per quarter cycle)

M \ α	α_1	α_2	α_3	α_4
0.0	0.0000°	33.0000°	33.0000°	60.0000°
0.1	3.2952°	31.8182°	33.9360°	58.8317°
0.2	4.8306°	30.7788°	35.0081°	57.6623°
0.3	6.1077°	29.7325°	36.0671°	56.4880°
0.4	7.2537°	28.6769°	37.1100°	55.3045°
0.5	8.3112°	27.6081°	38.1323°	54.1053°
0.6	9.2961°	26.5206°	39.1258°	52.8809°
0.7	10.2111°	25.4053°	40.0760°	51.6147°
0.8	11.0481°	24.2476°	40.9531°	50.2758°
0.9	11.7847°	23.0212°	41.6881°	48.7941°
1.0	12.3701°	21.6714°	42.0746°	46.9654°

Table 3.8. Optimized switching angles for bipolar PWM scheme B in the three-phase inverter (even number of switching angles per quarter cycle)

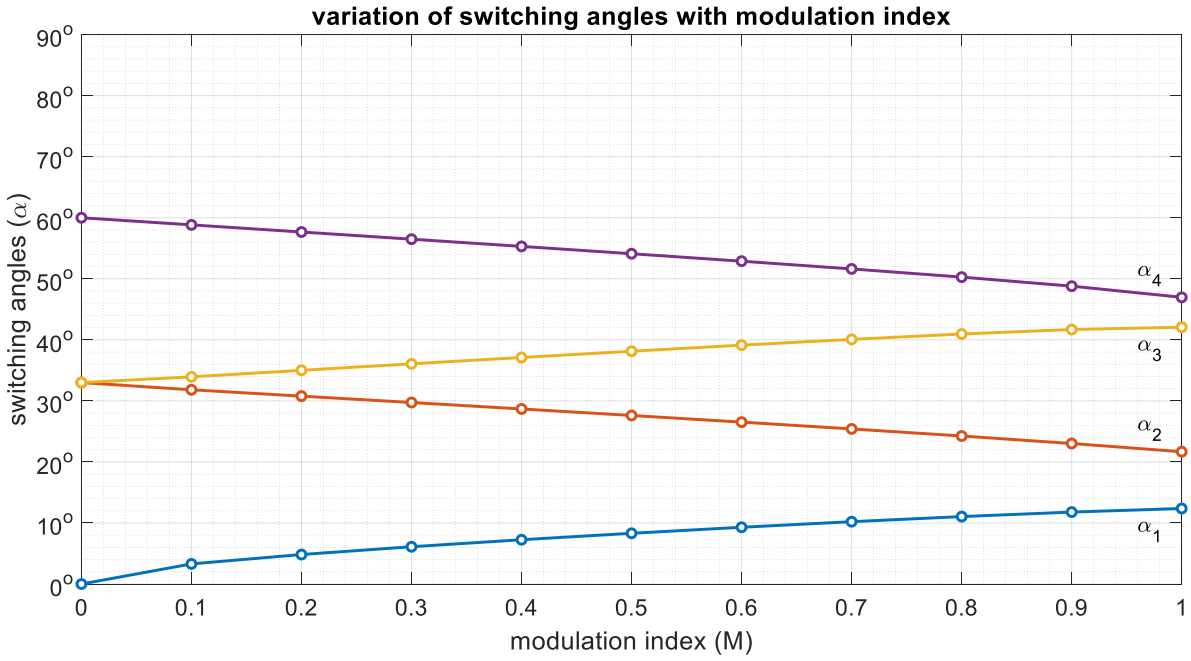

Figure 3.8. Optimized switching angles versus modulation index for PWM scheme B in the three-phase inverter (odd number of switching angles per quarter cycle)

Programmed PWM scheme	no. of switching angles (N)	Genetic Algorithm (no. of generations)	Sequential Quadratic Programming (no. of iterations)
bipolar scheme A for single phase inverter (odd *N*)	5	4	reaches local optimum only
bipolar scheme A for single phase inverter (even *N*)	4	5	converges (20 iterations)
bipolar scheme B for single phase inverter (even *N*)	6	7	reaches local optimum only
bipolar scheme B for single phase inverter (odd *N*)	5	25	reaches local optimum only
unipolar scheme for single phase inverter (odd *N*)	5	31	reaches local optimum only
unipolar scheme for single phase inverter (even *N*)	4	16	reaches local optimum only
Three phase inverter – scheme A (odd *N*)	5	6	reaches local optimum only
Three phase inverter – scheme B (even *N*)	4	5	converges (25 iterations)

Table 3.9. Comparison between Genetic Algorithm and Sequential Quadratic Programming Algorithm for obtaining solutions of selective harmonic elimination.

It is observed that the convergence of the gradient-based algorithm is marked by uncertainty. Gradient-based algorithms may or may not converge to the global optimum solution of the problem depending upon the starting point selected.

3.4 SUMMARY

The requirement of an evolutionary algorithm-based optimization approach to numerically solve for the switching angles for SHE in programmed PWM is discussed. The implementation of the genetic algorithm, an evolutionary algorithm is discussed. The global optimization problem of determining the optimized switching angles for various programmed

PWM schemes is formulated and solved using the genetic algorithm. The trend followed by the optimized values of the switching angles with respect to the modulation index is observed.

CHAPTER 4

CONCLUSIONS

The nonlinear transcendental equations associated with selective harmonic elimination in the output voltage waveforms of single-phase and three-phase VSI operated using programmed PWM schemes have been solved using the genetic algorithm. The genetic algorithm-based approach was successful in obtaining the global minimum solution to the optimization problem by successively improving the fitness values of the subsequent generations by means of the variation operators of recombination and mutation. The evolutionary algorithm-based optimization approach was found not to suffer from the drawbacks of the traditional gradient-based optimization approaches such as tedious computation steps, computational burden and convergence to local optima.

The solution of the switching angles for different values of the modulation index M obtained by the genetic algorithm may be pre-computed and stored to generate the required SHE PWM output voltage waveform in different applications. Though SHE-PWM output voltage waveforms have zero magnitude at low order harmonics that are specifically selected for elimination, there exist components at higher order harmonics. These higher order harmonics are easily filtered out using passive filters that do not significantly attenuate the fundamental component of voltage.

REFERENCES

[1] B. K. Bose, “Global Energy Scenario and Impact of Power Electronics in 21st Century,” in IEEE Transactions on Industrial Electronics, vol. 60, no. 7, pp. 2638-2651, July 2013.

[2] B. K. Bose, “The past, present, and future of power electronics [Guest Introduction],” in IEEE Industrial Electronics Magazine, vol. 3, no. 2, pp. 7-11, 14, June 2009.

[3] J. M. Carrasco et al., “Power-Electronic Systems for the Grid Integration of Renewable Energy Sources: A Survey,” in IEEE Transactions on Industrial Electronics, vol. 53, no. 4, pp. 1002-1016, June 2006.

[4] S. R. Bowes, “New sinusoidal pulse width modulated inverter,” *Proc. Inst. Electr. Eng.*, vol. 122, no. 11, pp. 1279-1285, Nov. 1975.

[5] T. C. Y. Wang, Zhihong Ye, Gautam Sinha and Xiaoming Yuan, “Output filter design for a grid-interconnected three-phase inverter,” Power Electronics Specialist Conference, 2003. PESC '03. 2003 IEEE 34th Annual, 2003, pp. 779-784 vol.2.

[6] P.N. Enjeti, P.D. Ziogas, J.F. Lindsay, “Programmed PWM techniques to eliminate harmonics - A critical evaluation”, Industry Applications Society Annual Meeting 1988. Conference Record of the 1988 IEEE, pp. 418-430 vol.1, 1988.

[7] D. B. Fogel, “What is evolutionary computation?,” in IEEE Spectrum, vol. 37, no. 2, pp. 26, 28-32, Feb 2000.

[8] K. F. Man, K. S. Tang and S. Kwong, “Genetic algorithms: concepts and applications [in engineering design],” in IEEE Transactions on Industrial Electronics, vol. 43, no. 5, pp. 519-534, Oct 1996.

[9] A. I. Maswood, S. Wei, and M. A. Rahman, “A flexible way to generate PWM-SHE switching patterns using genetic algorithm” in *Proc. IEEE APEC*, vol. 2, pp. 1130-1134.